NASA Contractor Report 191123

Shape Optimization of Tibial Prosthesis Components

D.A. Saravanos, P.J. Mraz, and D.T. Davy
Case Western Reserve University
Cleveland, Ohio

April 1993

Prepared for
Lewis Research Center
Under Grant NAG3–1027

NASA
National Aeronautics and
Space Administration

SHAPE OPTIMIZATION OF TIBIAL PROSTHESIS COMPONENTS

D.A. Saravanos,[1] P.J. Mraz,[2] and D.T. Davy[2]
Case Western Reserve University
Department of Mechanical and Aerospace Engineering
Cleveland, Ohio 44106

SUMMARY

NASA technology and optimal design methodologies originally developed for the optimization of composite structures (engine blades) are adapted and applied to the optimization of orthopaedic knee implants. A method is developed enabling the shape tailoring of the tibial components of a total knee replacement implant for optimal interaction within the environment of the tibia. The shape of the implant components are optimized such that the stresses in the bone are favorably controlled to minimize bone degradation, to improve the mechanical integrity of the implant/interface/bone system, and to prevent failures of the implant components. A pilot tailoring system is developed and the feasibility of the concept is demonstrated and evaluated. The methodology and evolution of the existing aerospace technology from which this pilot optimization code was developed is also presented and discussed. Both symmetric and unsymmetric in-plane loading conditions are investigated. The results of the optimization process indicate a trend toward wider and tapered posts as well as thicker backing trays. Unique component geometries were obtained for the different load cases.

Keywords: Optimization, Shape, Implants, Orthopaedic, Optimal Design, Knee, Prosthesis, Finite Element Analysis, Tibia.

---

[1]NASA Resident Research Associate at Lewis Research Center.

[2]Graduate Research Assistant and Professor, respectively.

1. INTRODUCTION

The history of the design of orthopaedic implants is best illustrated as an extensive, iterative process of design improvements by means of evolution. As a result, the technology and quality of these "human replacement parts" has soared to prodigious new heights over the past two decades. Particularly for total hip replacement (THR) and total knee replacement (TKR) implants (Fig. 1), designs have improved to the point where probabilities for tractable long-term survival rates and acceptable functional restoration are quite high. Nevertheless, even higher long-term success rates and longer potentially useful service lives are clearly very desirable goals.

The intricacies of optimizing any joint prosthesis design are most commonly defined in terms of structural mechanics. Although unacceptable clinical results can occur without structural failure, the predominant modes of implant failure may be described most directly and most often in terms of structural mechanics. Huiskes [1] has noted five possible design optimization objectives, all of which relate to possible structural failures in either the interface between implant component and adjacent bone, the adjacent bone itself, or the implant component itself.

Given that the prosthetic joint will satisfactorily reproduce gross joint dynamics, the goal of design optimization of orthopaedic implants becomes one of optimizing the shape and the material characteristics of the implant components to control stresses or some other related quantities in the structure. The satisfactory definition of the optimization criteria (objective function) can be a formidable task. However, once this is accomplished, the remainder of the design optimization process then becomes the laborious process of searching for the best corresponding choices for implant geometry and materials definition, especially for bony structures. The use of numerical non-linear programming techniques for this purpose has proven to be an extremely useful tool to the designer. Coupled with advanced structural analysis techniques, especially the finite element method (FEM), they have been used extensively with

considerable success in structural design [2].

Among the many contributions in the field, selectively mentioned is some of the work performed at the *NASA Lewis Research Center* on the multi-objective and multi-disciplinary optimization of laminated composite structures [3, 4], as it is related to the research described herein. This is presently adapted for prosthesis optimization. Applications of analogous optimal design methodologies in biomechanical design have been relatively few and limited in scope [1, 5-7]. Some recent work which has been conducted by applying the previously mentioned composite mechanics and structural optimization techniques to the design of the tibial component of TKR is also reported. The long-term goals are to develop some broadly applicable methodologies for optimizing the design of orthopaedic implants. The first efforts have been concentrated on examining the capabilities and limitations of these methods in application to shape optimization procedures in optimizing total knee prosthetic component shapes.

The methodology and the computer code are adapted from those used for the multi-disciplinary structural tailoring of composite structures [3, 4]. More specifically, the *Structural Tailoring of Advanced Turboprops* (STAT) [3] computer code was utilized. While there are many obvious differences in the applications, the combination of specific essential features, namely the composite mechanics, the finite element analysis, and the structural optimization techniques, remains the same. For the composite FEA models used in this research, laminated plate theories were applied. As a part of the study, the use of such models as a possible way to satisfactorily carry out the design optimization procedure without resorting to costly three-dimensional FEM models was examined and evaluated.

As a starting place, a pilot tailoring system is developed for the optimal design of the tibial component of the TKR. Specifically, we have considered the metal backed component with a central post or stem (Fig. 1), and have examined the shape tailoring of the post and the

thickness sizing of the metal backing or tray. Optimization parameters included the shape tailoring of the post and the thickness sizing of the metal backing tray. In our approach, we assume, as have others [1, 5-7], that the basic criterion for design optimization is the stress state in the bone/implant composite structure. For the tibial component, the most likely mode of failure is aseptic loosening, which involves the resorption of the bone adjacent to the implant. This is attributed in many cases to the stress-induced adaptation of the bone after the surgical procedure in response to the altered stress fields induced exclusively by the presence of the prosthetic implants. Thus, the optimal design goal becomes the minimization of undesirable bone atrophy of the adjacent bone, or, in a positive sense, the creation of favorable stress states in specific bone regions induced by the design of the TKR.

In this paper, we demonstrate the basic features of the methodology and document its evaluation as applied to the shape tailoring of the tibial component of a total knee prosthesis using this approach.

2. ANALYSIS OF BONES WITH LAMINATED STRUCTURE

The present section outlines the methods developed as NASA technology which, in turn, were used to model the quasi-static response of the upper tibia's laminated tissue structure. The overall procedure of these methods is outlined in Figure 2. The technology has been successfully applied to aerospace applications in the analysis of laminated composite blades, namely turbo-props, and other structures with anisotropic material layers [3, 8]. The methods have seen very limited application in the case of bone structures despite strong advantages and similarities; namely, the capability to represent non-uniform material regions of variable thickness and in-plane or out-of-plane bending/torsional deformations. Instead, most of the efforts have been focused either on two-dimensional finite element analyses based on plane-strain assumptions with thickness corrections to represent the inhomogeneity of the implanted tibia, or on elaborate three-dimensional analyses incorporating continuum solid element approaches. The laminate theory proposed herein may be viewed as a compromise between these two approaches.

The analysis basically involves three stages. In the first stage, the stiffness matrices representing the characteristics of the discrete bone layers are synthesized. Integration through the sagittal plane (thickness) provides the equivalent local through-the-thickness extensional and flexural stiffness matrices of the laminate properties, relating the generalized (average) plate stresses to the generalized (average) plate strains. In the second stage, the global static response is obtained with finite element analysis in the form of discretized nodal displacements in the frontal plane. The third and final stage involves the back-calculation of stresses within the bone and the implant components from the displacement field or global structural response. The generalized strains of the frontal plane are calculated followed by the calculation of the strains of each discretized layer. The stresses at the discretized material layers are then calculated from the layer strains.

2.1 Layer Stiffness

Assuming elastic materials and a plane-stress state at each discretized material, the layer stress $\{ \sigma_l \} = \{ \sigma_{lxx}, \sigma_{lyy}, \sigma_{lxy} \}$ is related to the layer strain $\{ \epsilon_l \} = \{ \epsilon_{lxx}, \epsilon_{lyy}, \epsilon_{lxy} \}$ through the layer stiffness matrix $[Q_l]$.

$$\{ \sigma_l \} = [Q_l] \{ \epsilon_l \} \tag{1}$$

The elements of matrix $[Q_l]$ for the case of an orthotropic material with the coordinate axes coinciding to the axes of material orthotropy are [8]:

$$[Q_l] = \begin{bmatrix} \frac{E_{l_{11}}}{1-\nu_{l_{12}}\nu_{l_{21}}} & \frac{E_{l_{11}}\nu_{l_{21}}}{1-\nu_{l_{12}}\nu_{l_{21}}} & 0 \\ \frac{E_{l_{11}}\nu_{l_{21}}}{1-\nu_{l_{12}}\nu_{l_{21}}} & \frac{E_{l_{22}}}{1-\nu_{l_{12}}\nu_{l_{21}}} & 0 \\ 0 & 0 & G_{l_{12}} \end{bmatrix}$$

where:

$E_{l_{11}}$ = *Longitudinal modulus*
$E_{l_{22}}$ = *Transverse modulus*
$\nu_{l_{12}}$ = *Poisson ratio*
$\nu_{l_{21}}$ = *Poisson ratio*
$G_{l_{12}}$ = *In-plane shear modulus*

The reduction of the stiffness matrix $[Q_l]$ in the case of isotropic materials is trivial. When the global coordinate axes do not coincide with the material orthotropy axes, then the stiffness matrix $[Q_l]$ is transformed into a full populated matrix $[Q_c]$ [8].

2.2 Laminate Stiffness

Based on Kirchoff's assumptions for extension and bending (plane sections through-the-thickness remain plane, and the interlaminar shear stresses are negligible), the layer strains are

related to the generalized strain of the section as follows:

$$\{ e_l \} = \{ 1, z \} \{ \epsilon^o, k \}^T \tag{2}$$

where $\{\epsilon^o\}$ is the mid-plane strain and $\{ k \}$ is the mid-plane curvature and they both represent the generalized strain of the laminate.

Combination of eqs. (1) and (2) and integration through-the-thickness provides the stiffness relation between the generalized force $\{ F \} = \{ N, M \}$ acting on the laminate and the generalized strain:

$$\{ N \} = [A]\{\epsilon^o\} + [C]\{ k \} \tag{3.a}$$

$$\{ M \} = [C]\{\epsilon^o\} + [D]\{ k \} \tag{3.b}$$

where $\{ N \} = \{ N_x, N_y, N_{xy} \}$ are the in-plane normal and shear forces and $\{ M \} = \{ M_x, M_y, M_{xy} \}$ are the bending and torsional moments, respectively. [A], [C], and [D] are the extensional, coupling, and flexural stiffness matrices, respectively, and are related to the layer stiffness matrix and the laminate configuration:

$$\{ [A], [C], [D] \} = \sum_{k=1}^{N_l} [Q]\{ t_k, t_k\overline{z_k}, t_k(\overline{z_k^2} + \frac{t_k^2}{12}) \} \tag{4}$$

where t_k is the thickness of the material and $\overline{z_k}$ is the distance from the centroid of the material to the midplane. In the case of symmetric laminations, such as the tibia configuration assumed in this research, the extension-flexure couple is negligible, $[C] = 0$, and eqs. (3.a) and (3.b) are decoupled. In the case of symmetric bone structures not acted upon by out-of-plane loads, the previously stated theory is reduced to the familiar plane strain models, however, it maintains the capability to represent the material inhomogeneity.

2.3 Finite Element Analysis

A two-dimensional triangular plate element was used to model the global static response

of the implanted tibia in the frontal plane. The element incorporates linear shape functions for the in-plane displacements and cubic shape functions for the out-of-plane displacements [9]. If $[\ B_s\ ]$ represents the strain shape function matrix relating the generalized strain $\{\ \epsilon\ \}$ to the discretized nodal displacements of the element $\{\ u_e\ \}$,

$$\{\ \epsilon\ \} = [\ B_s\ ]\{\ u_e\ \} \tag{5}$$

then the element stiffness matrix $[\ K_e\ ]$ will have the form:

$$[\ K_e\ ] = \int_A [\ B_s\ ]^T [\ K_L\ ][\ B_s\ ] dA \tag{6}$$

where: $[\ K_L\ ] = \begin{bmatrix} [A] & [C] \\ [C] & [D] \end{bmatrix}$

The element stiffness includes both in-plane and bending stiffness terms, hence, it can handle in-plane forces and out-of-plane moments. This type of laminate plate element provides a compromise between the restrictive, simplistic plane-strain elements and the computationally expensive, three-dimensional elements. In view of the extensive utilization of two-dimensional finite element analysis in the design of prosthetic components, the use of the laminated plate element appears well justified. To further reinforce this assumption, comparisons were performed between solutions obtained by the laminated plate element and a three-dimensional continuum element. The obtained results were very favorable and the verification is presented in subsequent sections of this paper.

2.4 Layer Stresses

Eq. (5) is used to calculate the generalized strain in each element from the discretized displacement field. The strains at each layer through-the-thickness are calculated using eq. (2). The layer stresses are finally back-calculated from eq. (1). These layer stresses are used as the

primary focus of the optimization code to achieve minimization of the desired objective function. Post processing capabilities have also been written in to the existing pilot tailoring code to allow for visual evaluation and stress plots of the aforementioned element stresses.

3. OPTIMAL IMPLANT DESIGN

The objective of the proposed shape optimization and design procedure is to control the stress field in the cortical and cancellous bones of the implanted tibia by changing the shape and the dimensions of critical implant components. Specifically, by iteratively evolving the shape of the post and the thickness of the metal backing-tray throughout the optimization process and performing finite element analyses at each design point, the behavior of the stress fields within the bone structure for a particular iteration can be observed. That information, obtained at each design point can then be used to direct the next design move in an effort to reach the optimum design by minimizing the objective function.

The shape optimization of elastic structures as a means to control the stresses and strain energy state of the structure has been an area of vigorous research in the last two decades, however, the optimal design of orthopaedic implants problem differs in many aspects and requires additional consideration. Some of the most profound differences include: (1) the complex performance criteria, and (2) the fact that we are working with a living, adaptive material in the bone tissues; a material which can change its mechanical properties continuously.

It is a well known fact that every healthy tibia has a unique bone macro- and micro-morphology that "efficiently" carries the applied loads at the joint. Research indicates [10-14] that this particular bone morphology develops in response to an average stress/strain related stimulus induced by the applied joint loads resulting in an optimum minimum-weight configuration of the bony structure. The bone adapts its morphology as a way of reacting to this stress stimulus. That is, bone is very similar to muscle tissue in the body in the way it behaves in response to usage. If a particular muscle is not used (stressed) it atrophies. The same reaction is true of bone. The presence of the prosthesis in the tibia drastically alters both the global mechanical characteristics and the load path in the now modified knee joint system. Hence, it

significantly perturbs the stress field in the cancellous bony tissues instituting the potential for changes in the bone which may cause undesirable bone atrophy and/or resorption in the vicinity of the bone-implant boundaries. The resorption of bone at the implant/bone interfaces is an extremely undesirable phenomenon in knee prostheses since it is primarily responsible for the typical failure mode in this joint. That is, the loosening and subsequent failure of the tibial component is a direct consequence of this bone atrophy or resorption. More specifically, by altering the stress state within the implanted tibia as a result of the presence of the TKR, unfavorable bone resorption can occur in areas of the tibia thought to be critical for good fixation as a direct result of implant geometry. Although, the exact physical mechanisms that stimulate bony ingrowth are not completely understood nor have they been quantified, they continue to be a subject of continuous research. It does seem apparent that the most important requirements for implant stability and long-term durability as related to fixation are directly related to the manipulation of the stresses near the bone/implant interfaces.

Bone remodeling has also been observed in areas away from the bone/implant interfaces within the tibia in response to the different stress patterns induced by the introduction of a TKR to the environment of the knee joint. As a result, areas experiencing bone atrophy (states of lower stress than in the normal skeleton) and areas of higher bone density (higher stress) may be developed. This type of global bone adaptation, may not as clearly or directly result in the failure of a prosthetic implant, however, it is an undesirable change and should be kept to a minimum. There are two reasons for this: (1) it alters the morphology and the original properties of the bone; and (2) if this global adaptation does occur, the design of the implant components will no longer be "optimal" because the underlying analysis to produce those designs would have been based on the original bone morphology. Therefore, it is also desirable to maintain the global stress field in the implanted tibia as near as is possible to normal physiological conditions.

Based on experimental results and clinical observations, phenomenological models have been developed to the point where one can attempt numerical predictions of bone remodeling histories [10, 11]. However, considerable work remains in order to validate the various models, and the appropriate parameters to be incorporated into these models are still to be determined experimentally. Hence, optimizing prostheses design using time dependent remodeling is relatively impractical for the iterative design process at the present time. The alternative approach, using a stress- or strain-related criterion, has a direct relationship to the anticipated remodeling behavior since they are typically the basis for the remodeling models [12-14]. The use of a stress-based criterion, although it does not follow the history of the remodeling process nor does it reflect the time dependent adaptation of the supporting medium, is nevertheless sufficient for a first approach to the design of an optimal prosthetic implant.

It appears that the most important requirements are minimal interfacial movement and moderate bone stresses/strains near the bone/implant interfaces [13, 15]. The global stress field in the implanted tibia should be also maintained within normal physiological levels. In this way, global alterations of the bone tissue will be restricted to a minimum level.

There are other secondary modes of implant failures which may be either mechanical failure of the implant components or bone fracture as a result of high stress concentrations in extreme loading conditions. Although preliminary finite element analyses indicate that the stress level in the bone and the implant are too low for this mode of failure, suitable preventive mechanisms have been incorporated into the proposed methodology to monitor this failure mode. That is, a primary check in the optimization process is that the chosen implant design will not fail mechanically as a result of the prescribed load case.

In view of the previous observations, candidate quantitative design criteria leading to favorable stress fields within the implanted tibia are: (1) minimization of the stress concentrations

at the vicinity of the bone/implant interface, and (2) maintenance of the stress in the bone within the physiological levels of the original tibia. Some additional criteria involve the prevention of mechanical failures, bounds on the admissible shape for the tibial post and tray, and minimal removal of bone tissue.

In this initial investigation of the problem, it is best to formulate the optimum design problem as the minimization of a single objective function:

$$\min \; (\; F(z) \;) \tag{7}$$

subject to lower and upper bounds on the design vector z and inequality constraints $G(z)$:

$$z^L \preceq z \preceq z^U \tag{8}$$

$$G(z) \preceq 0 \tag{9}$$

Based on the research performed by Carter and co-workers [14], the stress stimulus has been assumed directly proportional to the specific normalized von Mises distortion energy $H(\sigma)$:

$$H(\sigma) = (\frac{\sigma_{xx}}{S_{xx}})^2 + (\frac{\sigma_{yy}}{S_{yy}})^2 + (\frac{\sigma_{xy}}{S_{xy}})^2 - \frac{\sigma_{xx}}{S_{xx}}\frac{\sigma_{yy}}{S_{yy}} \tag{10}$$

It is desirable to control the von Mises distortion energy at the vicinity of the implant as well as throughout the rest of the tibia bone structure. In the rest of this paper, the subscripts g and d will indicate global and local stresses, respectively. The superscripts i and o will represent an implanted tibia and an unimplanted tibia, respectively. In this context, the proposed objective function is the minimization of the maximum specific distortion energy near the bone/implant interface H_d^i:

$$\min \{ \max \; H_d^i \} \tag{11}$$

subject to side constraints, eq. (8), constraints on the discretized cross-sectional areas A_i of the tibial post for admissible taper,

$$1 - \frac{w_{j+1}}{w_j} \preceq 0 \tag{12.a}$$

where w_j is the width of the post at a nodal line and w_{j+1} is the width of the post at a proximally

adjacent nodal line; stress failure constraints expressed in the form of distortion energy criterion,

$$H_g^i - 1 \leq 0 \tag{12.b}$$

and possible bounds on the deviation of the stresses between the implanted/unimplanted tibias,

$$\epsilon_l \leq H_g^i - H_g^o \leq \epsilon_u \tag{12.c}$$

The proposed objective function and constraints are converted to the form of standard non-linear programming equations, eqs. (7-9), as follows:

$$\min(\zeta) \tag{13}$$

subject to constraints, eqs. (8, 12.a,b,c), and additional constraints of the form:

$$\{ H_d^i \} \leq \zeta \tag{14}$$

where superscript i represents the discretized von Mises stress residuals at the vicinity of the bone/implant interface.

This constrained optimization problem is then solved numerically with the modified feasible directions non-linear programming method [16]. The feasible directions method is a direct search algorithm performing direct search in the feasible design domain. The algorithm incorporates a series of iterative steps until there is convergence to a local optimum within a prescribed tolerance. Each step involves the calculation of the objective function at the starting point, estimation of a search direction from the gradients of the objective function and the active constraints, and a subsequent line search along the search direction based on a polynomial interpolation. Convergence is obtained when the absolute or relative changes of the objective function at subsequent steps are less than prescribed tolerance limits.

The final output at this point quantifies changes that are necessary to be made to the initial or reference implant design to achieve an optimal design that is specific to that particular load case. Seemingly, it is therefore possible that an infinite number of "optimal" designs could be calculated simply by evaluating an infinite number of load cases for a given initial situation. In

light of this, it becomes obvious that it is necessary to more directly and clearly measure and quantify the joint reaction forces in a particular joint as well as be able to predict the stress state that will be imposed on the joint after implantation so that these scenarios can be evaluated. This will ensure that a truly optimal design has been achieved.

4. APPLICATION AND RESULTS

The present section includes evaluations demonstrating the applicability of the tailoring system on the shape optimization of a single-post tibial component (Fig. 1) subject to symmetric and unsymmetric loading in both the frontal and transverse planes. The section also describes the geometry and material properties and the validation of the FEA model.

4.1 Geometry and Material Properties

Typical dimensions and bone morphology representing the upper tibia of an average adult male were assumed in this study. For simplicity, symmetry was assumed in both frontal and sagittal planes, as well as, elliptical cross-sections. Nevertheless, the developed pilot tailoring system entails the capacity to handle more complicated bone geometries and morphologies. The variation in bone material properties was approximated by discrete laminated material regions and properties as shown in Fig. 3. As seen in Fig. 3, the discretized bone morphology consists of cortical bone surrounding different densities of cancellous bone.

The tibial component of the prosthetic knee implant, which was used both as a reference and an initial design, is a simple but valid representation of ones found to be in common use today and therefore it is a suitable start for the optimization process. The reference design incorporates a 15 mm thick ultra-high molecular-weight polyethylene (UHMWPE) plateau supported by a 3 mm thick titanium backing tray. A 15 mm by 15 mm square by 30 mm long titanium stem or post protrudes from the bottom center of the tray. The polyethylene plateau and the titanium backing tray are both 70 mm wide and 45 mm deep and they match exactly the geometry of the corresponding tibial cross-section.

4.2 Loading Conditions

Two different loading conditions were considered in this paper (Fig. 4):

(1) Symmetric, in-plane, vertical forces parabolically distributed over each condylar surface area totaling 2000 N. The load magnitude of 2000 N represents a resultant joint reaction force equivalent to three times the body weight, which is typical during normal, level walking [17, 18].

(2) Unsymmetric, in-plane, vertical forces totalling 1333 N and 667 N (2:1 ratio) respectively, parabolically distributed over their corresponding condylar surface. Unsymmetric loads are considered to be a more realistic representation of the actual loading conditions within the knee joint.

4.3 Validation of the FEA Model

In order to illustrate validity and limitations of the laminate plate theory used herein, results of the finite element analysis obtained from the laminate plate analysis were compared to results obtained from more detailed three-dimensional continuum finite element models. The comparisons made are for the reference prosthesis design described earlier subjected to both symmetric and unsymmetric in-plane loading conditions.

The two-dimensional, laminated plate model used in the optimization incorporated 220, three-noded, triangular elements. The three-dimensional model, used for validation only, incorporated 880, eight-noded, hexagonal solid elements and had approximately 5000 degrees of freedom. The applied loads of the three-dimensional model were equivalent to the vertical loads of the plate model, the only difference being that they were also parabolically varying through the thickness of each condylar surface.

There is good agreement in the von Mises stress between the two models, which is evident when comparing the stresses in each model for the cortical bone and cancellous bone regions as well as the tray and post configuration. While the stresses at every element are not exactly identical, the "trends" of the stresses in each model are significantly similar. That is, the general behavior of the stress contours in the three-dimensional model are adequately reproduced in the two-dimensional case for both symmetric and unsymmetric loading conditions.

4.4 Results

Corresponding to the requirement for maintenance of the bone/implant interface, we have chosen the objective function to be minimization of the maximum von Mises stress at the bone/implant interface regions.

The design variable sets for the optimization cases presented here involved combinations of post and tray geometry parameters including: the post length (-15% to +20%); the width of the post at several prescribed positions along its length (-25% to +25%); and tray thickness (-3% to +10%). The values in parentheses indicate the lower and upper bounds of allowed perturbations imposed as a percent of the respective reference implant design geometry. The post at all other positions was determined by cubic spline curve fits.

<u>4.4a In-Plane Loading, Symmetric.</u> Shape optimization of only the post resulted in a 26% reduction in the maximum strain within the cortical shell which occurs at the outermost elements in the tray/bone interface. For this design case, the post width has been thickened at the post/tray interface by 25% and then tapered while its overall length increased by 3%. The maximum stresses have been transferred toward the lower portion of the cortical bone as well (Fig. 5b).

Optimal sizing of only the tray thickness resulted in a 31% reduction in the maximum stress but does not transfer quite as much stress down the cortical shell as in the previous case. For this design case, the tray was thickened by 3%, illustrating that thicker trays provide improved immobilization at the tray/bone interface. The current trend of using metallic backing trays as opposed to the less successful all-plastic tibial implant configuration reinforces the obtained results.

Combined optimization of the post and tray resulted in a 30% reduction in the maximum stress and results in nearly the same stress distribution as in case 1. The tray has been thickened by 3% while the post has been tapered and shortened by less than 1% (Fig. 5c). Interestingly, the combined optimization did not produce additional reductions in the maximum stress. This was attributed to the fact that a stress state of equal maximum stresses at the lower end of the post and the outermost points of the tray was obtained with all designs which prevented further reductions.

Thus, the results for optimization in a symmetric loading scenario indicate the need for a design that includes a thicker holding tray with a wider but tapered post of slightly longer length as compared to the initial design case (Table I). Such a design transfers the maximum stress from the outer portions of the tray/bone interface region to regions below the bottom of the post within the cortical shell.

4.4b In-Plane Loading, Unsymmetric. Optimization of only the post resulted in a 15% decrease in the maximum stress within the implant/bone interface, and the maximum stress has now been transferred to elements in the cortical bone which are below the lower end of the post. The post has been shortened by 1%, as well as widened at the tray/post interface by 17% and then tapered (Fig. 6b). Fig. 6 also shows that the global maximum stress occurs at the boundary conditions

imposed at the bottom of the model and that this stress does not change significantly after optimization.

Optimization of only the tray thickness resulted in a 16% decrease in the maximum stress which occurs at the implant/bone interface. The tray has been thickened by 2%.

Combined optimization of the post and the tray resulted in a 18% reduction in the maximum stress within the implant/bone interface. In this case, the post has been shortened by 3% and tapered while the tray has been made thicker, 2%. The design combines the trends of the previous two cases, however somewhat different, and resulted in minor additional reductions (Fig. 6c).

Thus, the prosthesis optimization under unsymmetric loading indicates the need for a design that includes a thicker holding tray with a wider but tapered post of slightly shorter length as compared to the initial design case (Table II). Such a design results in the higher stresses appearing in regions that are below the bottom of the post.

5. SUMMARY

A method is developed for the optimization of orthopaedic knee implants by adapting NASA technology originally developed for the analysis and optimization of composite structures. The present paper is focused on the optimal design of the tibial implant components. The shape of the implant is tailored for improved bone growth near the boundaries of the implant. A research pilot code was developed to demonstrate the feasibility of the concept.

Evaluations of the pilot tailoring system were performed on the shape optimization of tibial implants subject to symmetric and unsymmetric distributed loads applied on the epiphyseal plate. The results illustrated that optimization of the implant shape can indeed reduce the

maximum stress in the bone at the vicinity of the implant and also produce more uniform stress distributions. Therefore, shape optimization techniques can be successfully applied in designing durable and customized knee implants. The applications illustrated that the optimization system is expected to provide the means for significantly improving knee prostheses and allowing for customized implant tailoring for each individual patient. The applications also demonstrated the dependence of the resultant optimal designs to the loads, suggesting the need for optimization under multiple loading conditions. The material properties of the implant were also proved important. Optimization of the material properties will be best accomplished with tailored composite implants, and work in this subject is currently in progress.

Acknowledgements -- This work is supported by the technology utilization office at the NASA Lewis Research Center, Cleveland, OH under NASA Grant NAG 3-1027.

REFERENCES

1. Huiskes, R.; Boeklagen, R.: Mathematical Shape Optimization of Hip Prosthesis Design. *J. Biomechanics*, vol 22, 1989, pp. 793-804.

2. Haftka, R.T.; Grandhi, R.V.: Structural Shape Optimization - A Survey. *Computer Methods in Applied Mechanics and Engineering*, vol 57, 1986, pp. 91-106.

3. Brown, K.; Harvey, P.: Structural Tailoring of Advanced Turboprops (STAT). NAS3-23941, 1987.

4. Saravanos, D.A.; Chamis, C.C.: Multi-Objective Shape and Material Optimization of Composite Structures Including Damping. *AIAA J.*, to appear. (Also NASA TM 102579, 1990.)

5. Huiskes R.; Boeklagen, R.: The Application of Numerical Shape Optimization to Artificial Joint Design. "Computational Methods in Bioengineering," (Spilker, R.L.; Simon, B.R., eds.) *BED*, vol 9, ASME, 1988, pp. 185-197.

6. Huiskes, R.; Kuiper, J.H.: Numerical Shape Optimization of Prosthetic Implants. *Proc. of the First World Congress of Biomechanics*, La Jolla, CA, 1990.

7. de Beus, A.M.; Hoeltzel, D.A.; Eftekhar, N.S.: Design Optimization of a Prosthesis Stem Reinforcing Shell in a Total Hip Arthroplasty. *J. biomech. Engng.*, vol 112, 1990, pp. 347-357.

8. Murthy, P.L.; Chamis, C.: Integrated Composite Analyzer (ICAN). NASA TP 2515, 1986.

9. Zienkiewicz, O.C.: The Finite Element Method, 3rd ed. McGraw-Hill Book Company (UK) Limited, 1977.

10. Hart, R.T.; Davy, D.T.; Heiple, K.G.: A Computational Method for Stress Analysis of Adaptive Elastic Materials With a View Toward Applications in Strain-Induced Bone Remodeling. *J. of biomech. Engng.*, vol 106, 1984, pp. 342-350.

11. Beaupre, G.S.; Orr, T.E.; Carter, D.R.: An Approach for Time-Dependent Bone Modeling and Remodeling--Theoretical Development. *J. Orthopaedic Research*, vol 8, no 5, 1990, pp. 651-661.

12. Cowin, S.C.; Hart, R.T.; Balsar, J.R.; Kohn, D.H.: Functional Adaption in Long Bones: Establishing *in-vivo* values for surface remodeling rate coefficients. *J. Biomechanics*, vol 18, 1985, pp. 665-684.

13. Huiskes, R.; Weinans, H.; Grootenboer, H.J.; Dalstra, M.; Fudala, B.; Sloof, T.J.: Adaptive Bone-Remodeling Theory Applied to Prosthetic-Design Analysis. *J. Biomechanics*, vol 20, 1987, pp. 1135-1150.

14. Carter, D.R.; Fyhrie, D.P.; Whalen, R.T.: Trabecular Bone Density and Loading History: Regulation of Connective Tissue Biology by Mechanical Energy. *J. Biomechanics*, vol 20, 1987, pp. 785-794.

15. Vasu, R.; Carter, D.R.; Schurman, D.J.; Beaupre, G.S.: Epiphyseal-Based Designs for Tibial Plateau Components--I. Stress Analysis in the Frontal Plane. *J. Biomechanics*, vol 19, 1986, pp. 647-662.

16. Vanderplaats, G.N.: A Robust Feasible Directions Algorithm for Design Synthesis. *Proc. 24th AIAA/ASME/ASCE/AHS Structures, Structural Dynamics, and Materials Conference*, Lake Tahoe, NV, 1983.

17. Morrison, J.B.: The Mechanics of the Knee Joint in Relation to Normal Walking. *J. Biomechanics*, vol 3, 1970, pp. 51-61.

18. Smidt, G.L.: Biomechanical Analysis of Knee Flexion and Extension. *J. Biomechanics*, vol 6, 1973, pp. 79-92.

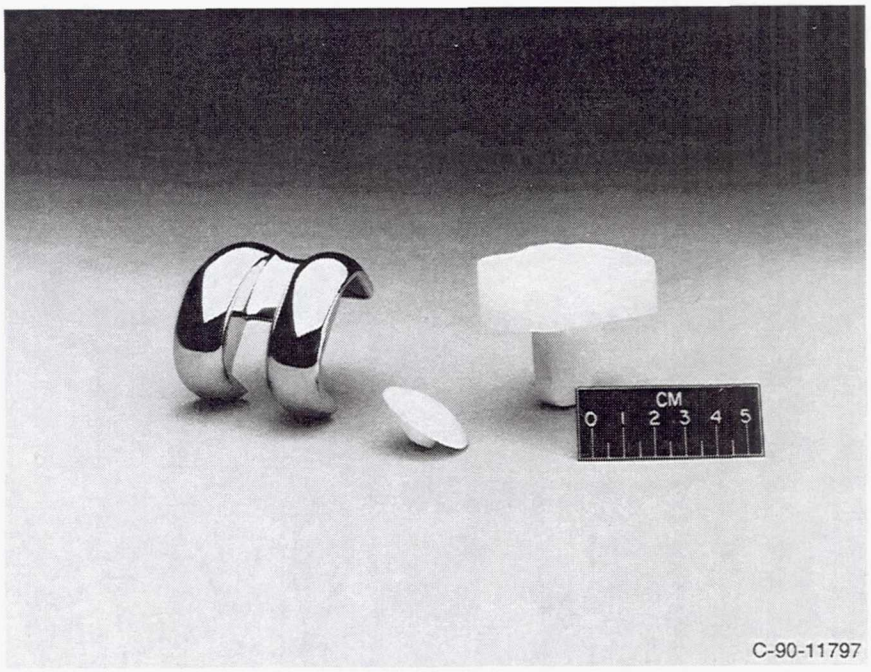

Figure 1.—Typical components of knee implants (from left to right): (a) Femoral component; (b) Patellar component; (c) Tibial component.

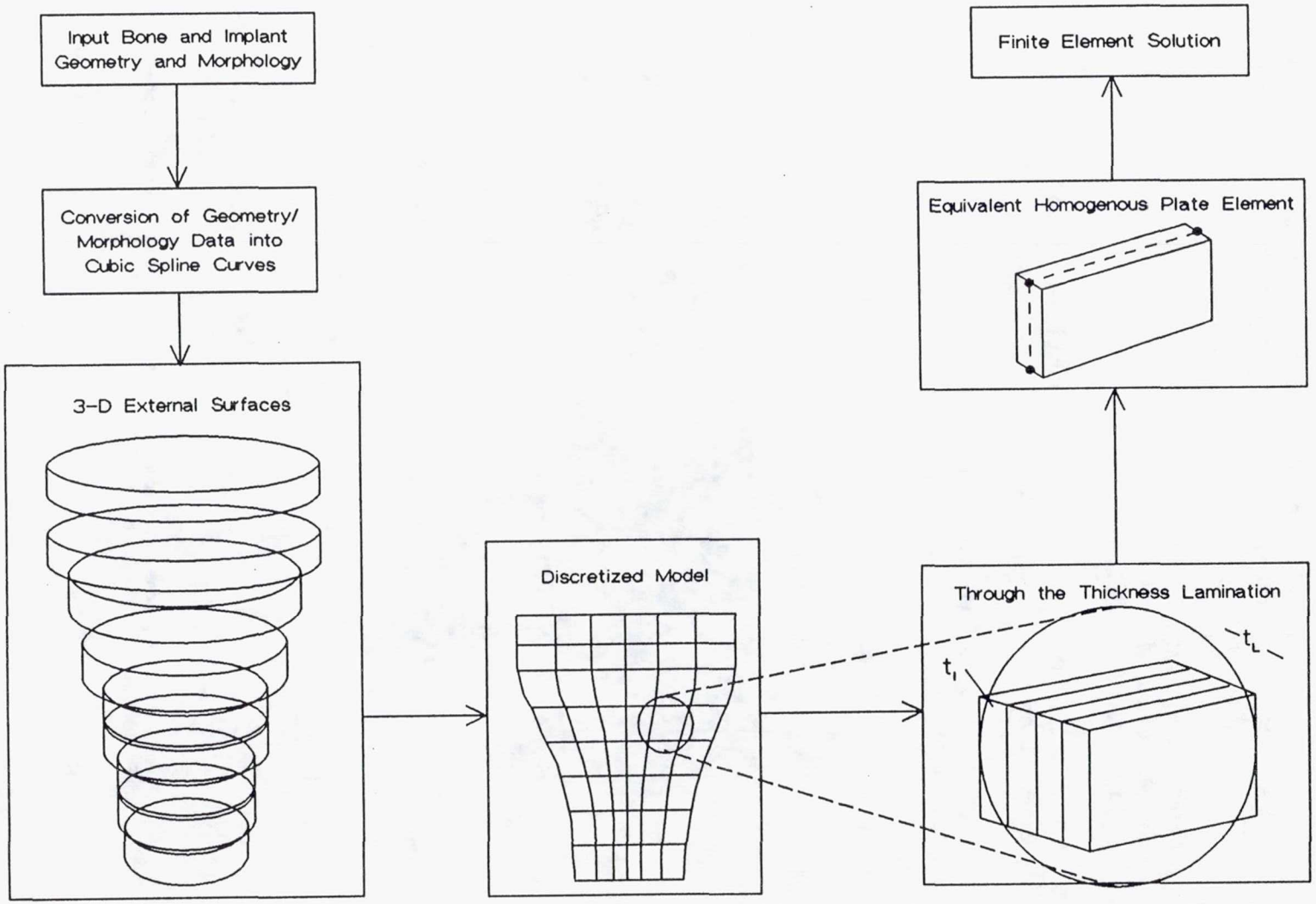

Fig. 2 Stages of the Laminate Plate Analysis.

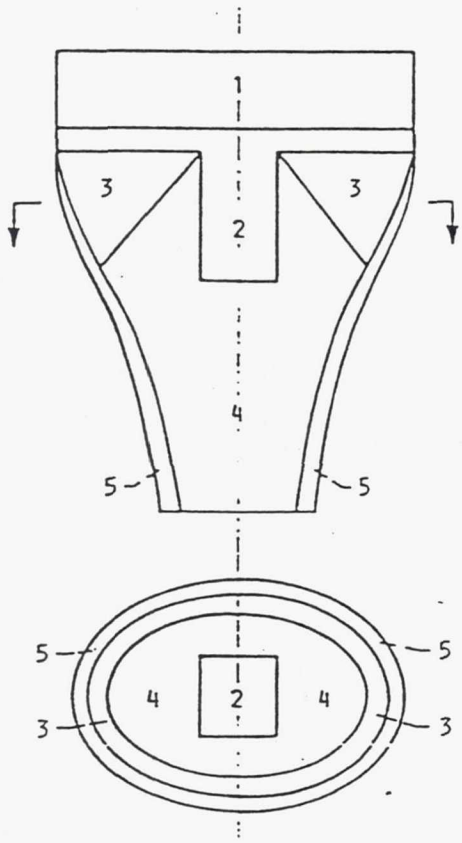

MATERIAL PROPERTIES FOR CORRESPONDING MATERIAL REGIONS

MATERIAL	DESCRIPTION	YOUNG'S. MPa	MODULUS. Mpsi	POISON'S RATIO
1	POLYETHYLENE	500	0.08	0.40
2	TITANIUM	113 764	16.50	0.30
3	CANCELLOUS HD	400	0.06	0.20
4	CANCELLOUS LD	200	0.03	0.20
5	CORTICAL SHELL	15 169	2.20	0.32

Fig. 3 Morphology and material regions for typical adult male tibia with prosthesis.

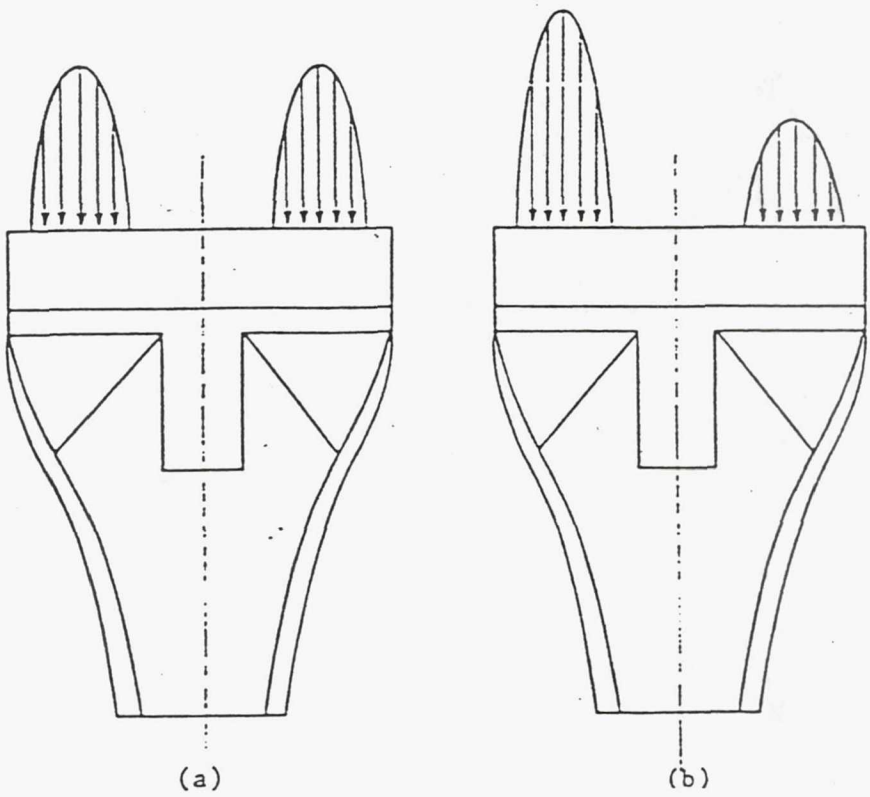

Fig. 4 Loading scenarios: (a) In-plane, symmetric; (b) In-plane, unsymmetric.

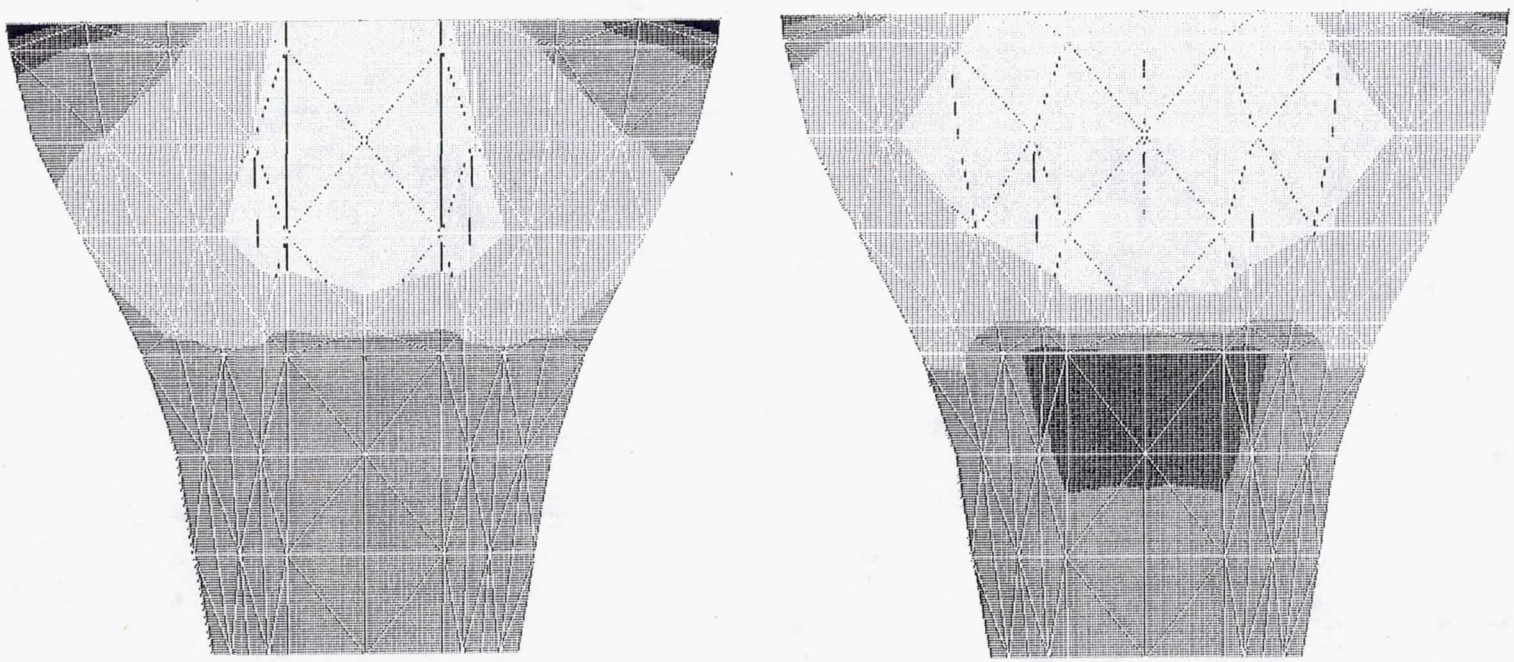

Fig. 5 Equivalent stress distributions in the cortical bone for symmetric loads: (a) Reference design; (b) Optimized post only.

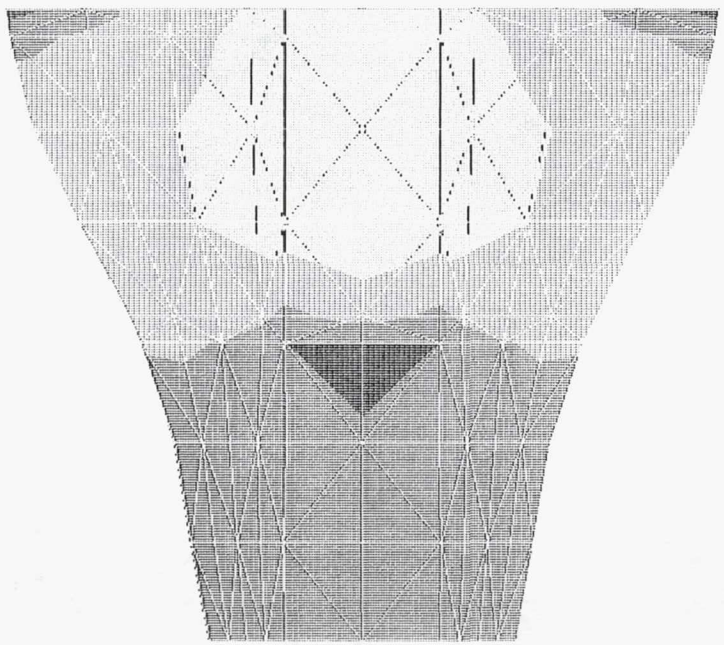

c)

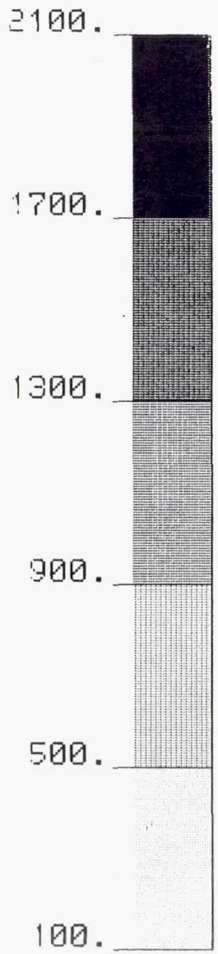

Fig. 5 (continued) (c) Optimized tray and post.

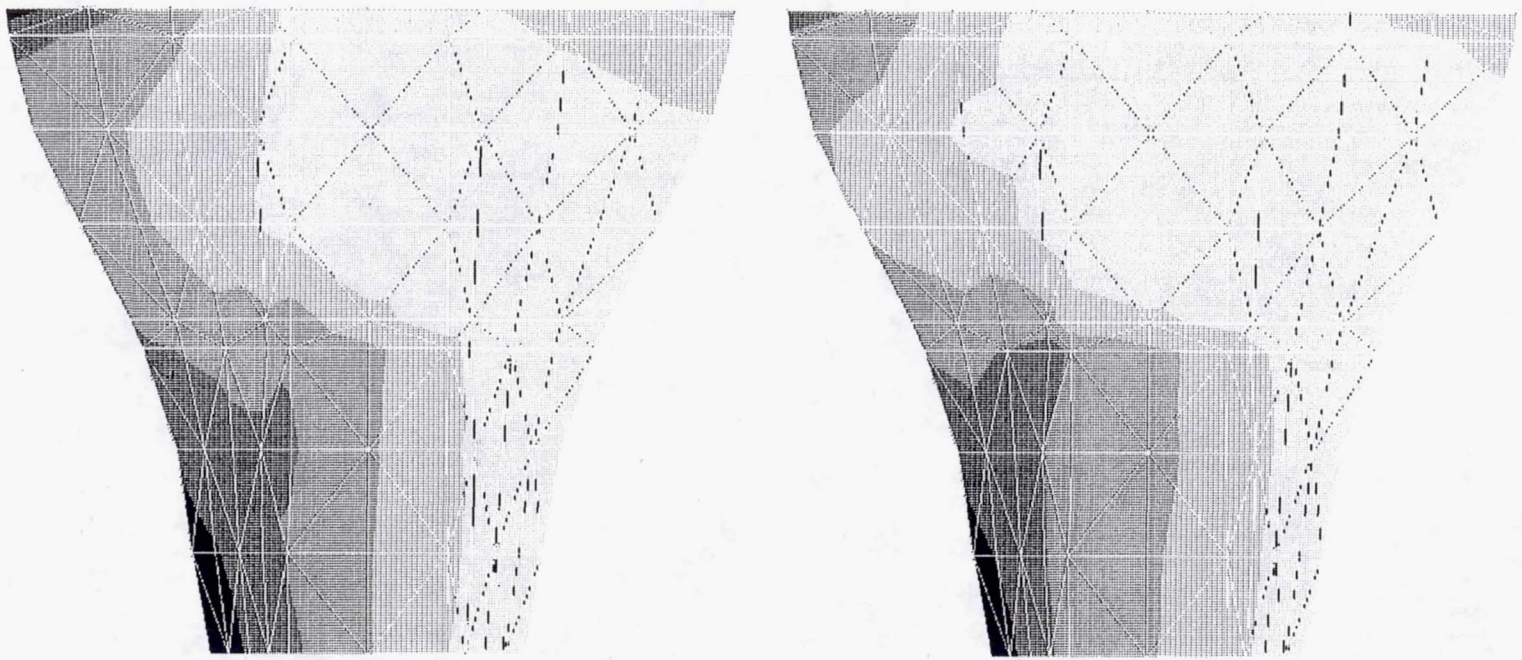

Fig. 6 Equivalent stress distributions in the cortical bone for unsymmetric loads: (a) Reference design; (b) Optimized post only.

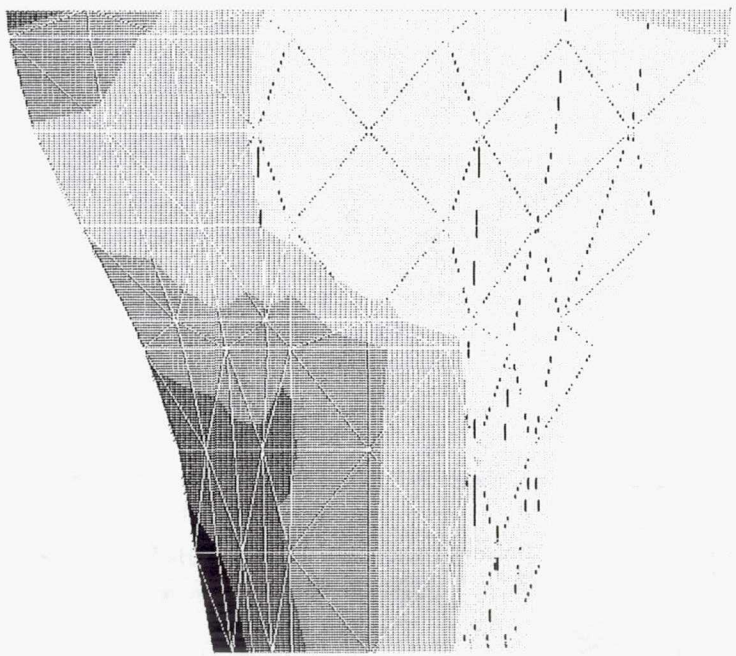

c)

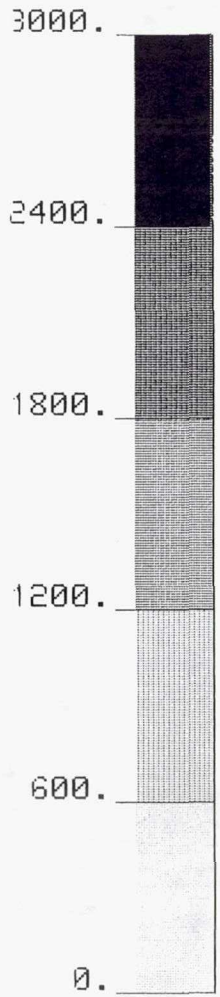

Fig. 6 (continued) (c) Optimized tray and post.

Table I. Results of Shape Optimization for Minimizing the Maximum von Mises Stress in the Interface Layer for Symmetric, In-plane Loading.

	Initial Design	Optimal Post	Optimal Tray	Optimal Tray/Post
Width @ Top of Post (mm)	15.0	32.5	(15.0)	18.0
Width @ Bottom of Post (mm)	15.0	15.7	(15.0)	15.6
Length of Post (mm)	30.0	32.2	(30.0)	29.9
Thickness of Tray (mm)	3.0	(3.0)	5.8	5.4
% Reduction of Obj. Function	***	26%	31%	30%

Table II. Results of Shape Optimization for Minimizing the Maximum von Mises Stress in the Interface Layer for Unsymmetric, In-plane Loading.

	Initial Design	Optimal Post	Optimal Tray	Optimal Tray/Post
Width @ Top of Post (mm)	15.0	27.9	(15.0)	16.6
Width @ Bottom of Post (mm)	15.0	16.0	(15.0)	16.2
Length of Post (mm)	30.0	29.4	(30.0)	27.6
Thickness of Tray (mm)	3.0	(3.0)	4.7	4.7
% Reduction of Obj. Function	***	15%	16%	18%

REPORT DOCUMENTATION PAGE

Form Approved
OMB No. 0704-0188

1. AGENCY USE ONLY (*Leave blank*)	2. REPORT DATE	3. REPORT TYPE AND DATES COVERED
	April 1993	Final Contractor Report

4. TITLE AND SUBTITLE

Shape Optimization of Tibial Prosthesis Components

5. FUNDING NUMBERS

WU–141–20–0F
G–NAG3–1027

6. AUTHOR(S)

D.A. Saravanos, P.J. Mraz, and D.T. Davy

7. PERFORMING ORGANIZATION NAME(S) AND ADDRESS(ES)

Case Western Reserve University
Cleveland, Ohio 44106

8. PERFORMING ORGANIZATION REPORT NUMBER

E–7815

9. SPONSORING/MONITORING AGENCY NAME(S) AND ADDRESS(ES)

National Aeronautics and Space Administration
Lewis Research Center
Cleveland, Ohio 44135–3191

10. SPONSORING/MONITORING AGENCY REPORT NUMBER

NASA CR–191123

11. SUPPLEMENTARY NOTES

D.A. Saravanos, P.J. Mraz, and D.T. Davy, Case Western Reserve University, Cleveland, Ohio 44106, and NASA Resident Research Associates, Graduate Research Assistants, and Professors of Mechanical and Aerospace Engineering at Lewis Research Center. Project Manager, D.A. Hopkins, (216) 433–3260.

12a. DISTRIBUTION/AVAILABILITY STATEMENT

Unclassified - Unlimited
Subject Category 51

12b. DISTRIBUTION CODE

13. ABSTRACT ***(Maximum 200 words)***

NASA technology and optimal design methodologies originally developed for the optimization of composite structures (engine blades) are adapted and applied to the optimization of orthopaedic knee implants. A method is developed enabling the shape tailoring of the tibial components of a total knee replacement implant for optimal interaction within the environment of the tibia. The shape of the implant components are optimized such that the stresses in the bone are favorably controlled to minimize bone degradation, to improve the mechanical integrity of the implant/interface/bone system, and to prevent failures of the implant components. A pilot tailoring system is developed and the feasibility of the concept is demonstrated and evaluated. The methodology and evolution of the existing aerospace technology from which this pilot optimization code was developed is also presented and discussed. Both symmetric and unsymmetric in-plane loading conditions are investigated. The results of the optimization process indicate a trend toward wider and tapered posts as well as thicker backing trays. Unique component geometries were obtained for the different load cases.

14. SUBJECT TERMS

Optimization; Shape; Implants; Orthopaedic; Optimal design; Knee; Prosthesis; Finite element analysis; Tibia

15. NUMBER OF PAGES
33

16. PRICE CODE
A03

17. SECURITY CLASSIFICATION OF REPORT	18. SECURITY CLASSIFICATION OF THIS PAGE	19. SECURITY CLASSIFICATION OF ABSTRACT	20. LIMITATION OF ABSTRACT
Unclassified	Unclassified	Unclassified	

National Aeronautics and
Space Administration

Lewis Research Center
Cleveland, Ohio 44135